Proceedings World Geothermal Congress 2026
Calgary, Canada, June 8 – 11, 2026

Flow modeling of a competing geothermal well with multiple feed zones and multiphase flow

Dimas T. Maulana[1, 4*], Farid M. Antoni[2], Tony Widiatmoro[3], Masoud Babaei[4*]
The University of Manchester[1*], Bandung Institute of Technology[2], Perusahaan Listrik Negara (PLN)[3], The University of Manchester[4]
E-mail: dimas.maulana@manchester.ac.uk; masoud.babaei@manchester.ac.uk

Keywords: Competing flow, multi-feedzone, coupled wellbore-reservoir simulation, geothermal well.

INTRODUCTION

Production well tests in geothermal fields quantify well productivity and flow capacity under specific reservoir and operating pressures, generating discharge curves that support design and performance monitoring (Moya *et al.,* 1998; Aragón *et al.,* 2008). When downhole measurements are limited, inflow performance relationships and coupled reservoir-wellbore models are used to infer flow contributions from multiple feed zones (Aragón *et al.*, 2008; Moya *et al.,* 1998; Xu *et al.,* 2017; Li *et al.,* 2021). Such coupling is particularly important for multiphase, multi-feed systems, where few simulators can represent the interaction between reservoir deliverability and wellbore hydraulics in a physically consistent manner (Hadgu *et al.,* 1995).

Cyclic ("coughing'') discharged behavior observed in several Taupo Volcanic Zone wells occurs despite stable surface flow-control conditions and is widely attributed to competing feed zones with contrasting pressures, enthalpies, and permeabilities (Grant & Bixley, 2011; Moon *et al.,* 2018). These oscillations arise from transient mass-energy coupling and changes in flashing depth and density structure within the wellbore (Grant *et al.,* 1979; Haukwa & O'Sullivan, 1981; Inagaki *et al.,* 2014; Shulyupin, 2017; Yanto *et al.,* 2019). Recent work has demonstrated the value of a coupled wellbore-reservoir simulation for diagnosing such field cases by explicitly capturing the consistent explanation of multiphase reservoir inflow and transient wellbore thermohydraulics (Moon *et al.,* 2018; Jiménez Martínez and Renner, 2022; Peng *et al.,* 2022).

Accordingly, this study reconstructs a multi-feed wellbore model for ULB-01 using a pressure-drop approach constrained by production test and PTS data, and integrates the inferred feed-zone conditions with reservoir simulation to interpret cycling under low-pressure operation. The workflow comprises: (1) steady-state wellbore reconstruction to estimate feed contributions; (2) sensitivity tests on key inputs (e.g., feed enthalpy/pressure and permeability); and (3) validation against field measurements to ensure consistency between simulated and observed responses.

1 WELL PROFILE

The pressure and temperature measurements of the well ULB-1 obtained during shut-in were assumed to represent the initial formation conditions in the potential feed zones (FZ). The PTS data from the second test have revealed the occurrence of fluid influxes, most prominently at depths of approximately 650, 950, and 1080 meters. Therefore, spinner-derived fluid velocities were used to calculate mass flow rates and estimate the productivity index (PI) of each feeding zone around these depths, as summarized in Table 1. These parameters then serve as a reference for subsequent flow modeling.

Table 1: Initial condition of each feed zone. The following data is taken from the PTS logging, which consists of pressure and temperature.

Parameters	FZ-1	FZ-2	FZ-3
Depth (meter)	650	950	1080
Reservoir Pressure (bar)	28	58	69
Reservoir Temperature (°C)	225	233	235

2 WELLBORE SIMULATION APPROACH

Previous studies on Well ULB-01 indicated a vapor-dominated upper zone and a liquid-dominated lower zone at temperatures of 230–240◦C (Kurniawan *et al.,* 2018), suggesting a complex two-phase feed structure. To characterize such systems, pressure–temperature–spinner (PTS) surveys are commonly employed to determine reservoir and flow characteristics. Shut-in PTS surveys establish initial reservoir pressure and temperature, while flowing PTS surveys provide pressure, temperature, and spinner data along the wellbore. Among these measurements, temperature and spinner logs are particularly effective for identifying feed zones and estimating their relative flow contributions (Grant & Bixley, 2011; Gudmundsdóttir & Steingrímsson, 2000). Using these logs, it is possible to estimate the mass flow rate by averaging pressure, temperature, and spinner data during logging runs (Buscato, 2012).

A geothermal wellbore simulator solves the conservation of mass, momentum, and energy for steady-state two-phase flow (McGuinness, 2013; Tonkin *et al.,* 2020). The pressure drop along the well is modelled as the sum of frictional, gravitational, and acceleration components. The frictional term depends on flow velocity, diameter, and fluid properties, while the elevation term is governed by fluid density and gravity. Under steady discharge conditions, the acceleration effect is relatively small and is therefore often neglected in wellbore analyses. The modified Hagedorn-Brown correlation is applied to estimate the pressure drop in the vertical two-phase flow (Saptadji *et al.,* 2023), while the separated flow conditions are modelled using the Harrison-Freeston method (Churchill, 1977; Freeston, 1980).

In the separated flow model with the assumption of annular flow, the total pressure drop is determined by the combined effects of friction and acceleration influencing the liquid film surrounding the gas core (Wallis, 1969; Hewitt and Hall-Taylor, 1970). The Hariston–Freeston method adopts a similar approach to the homogeneous model but incorporates an acceleration correction term that accounts for the changing momentum of the gas–liquid mixture as steam quality (mass fraction of vapor) varies along the flow (Harrison & Freeston, 1973). The key parameters that describe this interaction include the void fraction, phase velocities, and Reynolds number based on the liquid phase (Collier & Thome, 1994).

The void fraction, which represents the volumetric proportion of the gas phase within the flow, is a critical parameter affecting all other two-phase flow characteristics. According to the correlation proposed by Butterworth (1975), the void fraction α is explicitly related to the steam fraction x (mass fraction of vapor) and the specific volumes of the liquid (v_f) and gas (v_g) phases as:

$$\alpha(x) = \frac{1}{1 + \left(\frac{1-x}{x}\right)^{0.8} \left(\frac{vf}{vg}\right)^{0.515}}$$

The Reynolds number, based on the liquid-phase properties, describes the degree of turbulence and is used to determine the friction factor in the annular film region (Freeston, 1980). It is modified from the single-phase form to account for the reduced flow area occupied by the liquid film:

$$Re(x) = \frac{\dot{m}(1-x)D}{\mu_f A\big(1-\alpha(x)\big)}$$

Here, m is the total mass flow rate, D the pipe diameter, A the flow area, and μ_f the dynamic viscosity of the liquid. The presence of $(1-\alpha)$ in the denominator emphasizes that as the void fraction increases (more vapor, thinner liquid film), the effective velocity in the liquid film increases, leading to higher Reynolds numbers and possibly greater turbulence.

The pressure gradient combining friction and acceleration effects is derived by substituting the phase velocities and acceleration correction into the wall shear expression. Therefore, the final explicit form is:

$$\left(\frac{dP}{dZ}\right)_{fric+acc} = \frac{\lambda\, \rho_f \dot{m}^2}{2D\, A^2} \cdot \frac{(1-x)^2 v_f^2}{(1-\alpha)^2} \cdot \frac{1}{1 - \frac{\dot{m}^2 x^2 v_g}{P \alpha^2 A^2}}$$

In this equation, λ is the Darcy friction factor, ρ_f is the liquid density, and P is the local pressure. The void fraction $\alpha(x)$ appears explicitly, showing that the pressure gradient is highly sensitive to changes in vapor quality. As x increases, α increases rapidly, which reduces the liquid film thickness and generally increases the frictional and acceleration effects.

3 RESULT AND DISCUSSION

Although the wellbore flow model was initially developed , wellhead data exhibited fluctuating pressures and steam/brine flow rates. Consequently, a bottom-up approach was adopted, using PTS log data and precalculated productivity indices to replicate fluid flow from the feed zones to the wellhead. The reservoir enthalpy was assumed to depend on the temperature and pressure in the feeding zones, with reference pressures selected from FZ-3.

Following the previous step, wellbore simulations were performed to match the measured wellhead conditions. For high wellhead pressure (41 bar at FZ-3), enthalpy adjustments of 970, 930, and 2700 kJ/kg were applied to FZ-1, FZ-2, and FZ-3, respectively, yielding pressure drops consistent with PTS at test-1 (Figure 1a). Under low wellhead pressure (29.62 bar at FZ-3), the temperature profile indicated a cooler water influx at FZ-2, with an enthalpy decreasing from 930 to 740 kJ/kg, reflecting competing fluid flows from the formation (Figure 1b). These simulations capture the thermodynamic and hydraulic behavior of the drilled well, providing reliable input for reservoir modeling and improving understanding of feed zone performance under varying operating pressures.

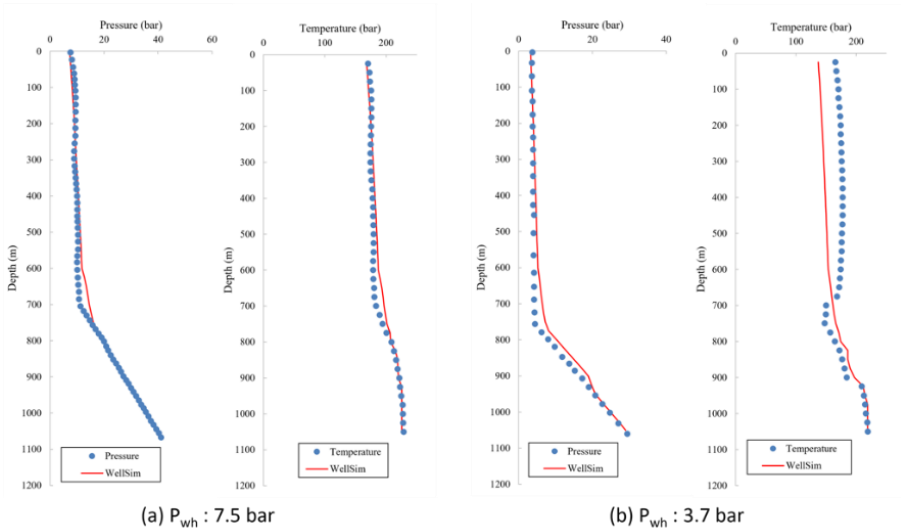
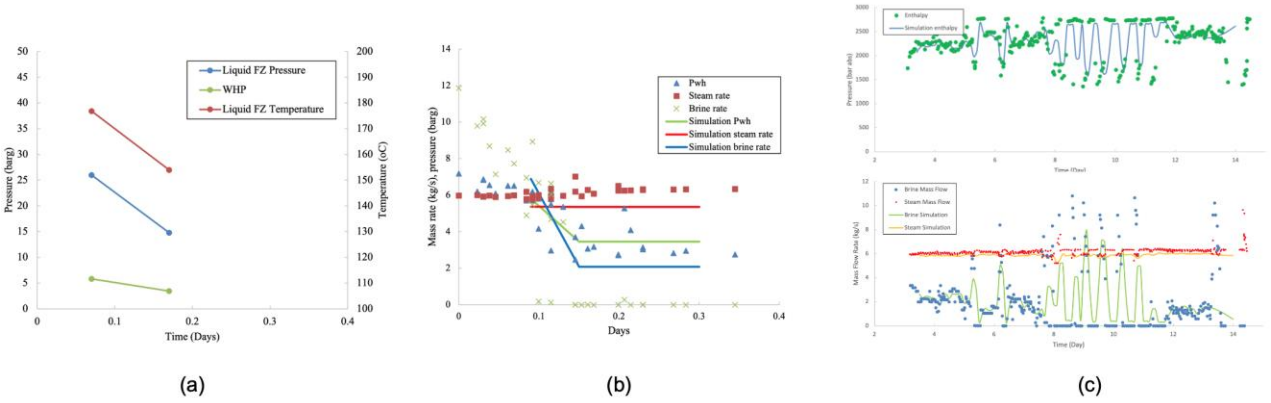


Figure 1: The wellbore simulation results (red line) are compared with the well flow data (blue dots) for high wellhead pressure (a) and low wellhead pressure (b) conditions.

The reservoir simulation focuses on the cold-water breakthrough under low-pressure conditions. Recent studies (Kurniawan *et al.,* 2018; Hammad & Sutopo, 2025) suggest a lower temperature zone near the southwest boundary of ULB-1, potentially allowing cold-water inflow when the bottomhole pressure (P_{wf}) drops. Due to limited downhole data available, wellbore simulation is used to estimate pressure and temperature at the feed zones.

Figure 2a shows that the wellbore model, constrained by the flowing PTS survey, is used to infer liquid-feedzone pressure and temperature under both high and low WHP conditions. Figure 2b compares measured wellhead pressure and phase mass rates with the corresponding wellbore-simulation outputs, indicating that the model captures the key production trends. Using these inferred feedzone inputs, the coupled TOUGH2–wellbore simulation reproduces the main surface responses (Figure 2c) and agrees well with production data. The simulated mean wellhead pressure (9–11 bara) is matched within ±10–15% during stable periods, while the steam mass flow remains near 6 kg/s with typical deviations below 10%. This level of agreement is consistent with prior coupled reservoir–wellbore studies showing that integrating wellbore hydraulics with reservoir deliverability improves the fidelity of surface-pressure and flow predictions in multi-feed geothermal systems (Hadgu et al., 1995; Peng et al., 2022), and aligns with the use of IPR-style relationships as a practical benchmark for geothermal deliverability under constrained measurements (Moya et al., 1998; Aragón et al., 2008). Produced enthalpy is also captured within 2200–2700 kJ/kg with mostly <10% deviation under steady conditions, suggesting that the model preserves the dominant energy balance and phase-partitioning behavior expected for geothermal wellbore flow when energy conservation and two-phase thermodynamics are treated consistently (McGuinness, 2013; Grant & Bixley, 2011). Although short-term brine surges are smoothed, the overall match demonstrates that the coupled workflow reliably translates reservoir deliverability into realistic surface production behavior. According to prior studies on cycling/instability in geothermal wells, the remaining mismatch in rapid liquid transients likely reflects short-timescale two-phase flow regime dynamics (e.g., intermittent holdup and flashing-depth migration) that are difficult to reproduce with quasi-steady or averaged

boundary representations and simplified flow-regime closures (Grant et al., 1979; Haukwa & O'Sullivan, 1981; Shulyupin, 2017; Moon et al., 2018).



(a) (b) (c)

Figure 2: (a) Liquid feedzone pressure and temperature inferred from PTS-constrained wellbore modeling under high and low WHP. (b) Measured versus simulated wellhead pressure and phase mass rates. (c) Coupled TOUGH2–wellbore match to surface wellhead pressure, phase rates, and produced enthalpy.

CONCLUSION

This study reconstructed and validated a multi-feed wellbore model for geothermal well ULB-01 in the Ulumbu geothermal field using a pressure-drop approach constrained by flowing PTS and production data. The inferred feed-zone boundary conditions model was subsequently coupled with a TOUGH2 reservoir model to determine cyclic behavior under low wellhead pressure conditions. Three dominant feed zones were identified at approximately 650, 950, and 1080 m depth. The bottom-up wellbore reconstruction indicates that the intermediate feed zone (FZ-2) experiences cooling and a reduction in inferred enthalpy during low-pressure operation, suggesting competing inflow and potential cold-water contribution. The coupled TOUGH2–wellbore simulations successfully reproduce the main surface observations, matching mean wellhead pressure, mass flow, and produced enthalpy. These findings demonstrate that the coupled wellbore–reservoir modelling is essential to translate feed-zone thermodynamic evolution into surface constraints and phase split, providing a robust framework for diagnosing unstable discharge and evaluating low-pressure operating strategies in multi-feed geothermal wells.

Acknowledgements

The first author acknowledges the Center for Higher Education Funding and Assessment (PPAPT), the Ministry of Higher Education, Science, and Technology (Kemdiktisaintek), and the Indonesia Endowment Fund for Education (LPDP) for their financial support through the Indonesian Education Scholarship (BPI) doctoral program (Grant No. 0967/J5.2.3/BPI.LG/VIII/2022). The authors also extend their sincere gratitude to the UNIMUS team at the University of Manchester.

REFERENCES

Aragón, A., Moya, S. L., & García-Gutiérrez, A. (2008). Inflow performance relationships in geothermal and petroleum reservoir engineering: A review of the state of the art. Geothermics, 37(6), 635–650.

Buscato, N. M. (2012). Quantifying feed zone contributions from pts data and pressure transient analysis using welltester. Proceedings 3rd International Geothermal Conference, Philippines, 1–6.

Butterworth, D. (1975). A comparison of some void-fraction relationships for co-current gas-liquid flow. International Journal of Multiphase Flow, 1, 845–850.

Churchill, S. W. (1977). Friction factor equation spans all fluid-flow regimes. Chemical Engineering Journal, 84, 91–92.

Collier, J.G. and Thome, J.R., 1994. *Convective boiling and condensation*. 3rd ed. Oxford: Oxford University Press.

Freeston, D. H. (1980). A comparison of experimental results of pressure drop for two-phase steam/water and air/water mixtures in a horizontal pipe. 7th Australian Hydraulics and Fluid Mechanics Conference.

Grant, M. A., & Bixley, P. F. (2011). Geothermal reservoir engineering (2nd ed.). Elsevier.

Grant, M. A., Bixley, P. F., & Syms, M. C. (1979). Instability in well performance. Geothermal Resources Council Transactions, 3.

Gudmundsdóttir, V., & Steingrímsson, B. (2000). Geothermal well logs: The role of spinner, temperature and pressure logging during drilling in locating feed zones. Proceedings World Geothermal Congress, 767–772.

Hadgu, T., Zimmerman, R. W., & Bodvarsson, G. S. (1995). Coupled reservoir-wellbore simulation of geothermal reservoir behavior. Geothermics, 24(2), 145–166.

Hammad, F. K., & Sutopo. (2025). Updated reservoir model of ulumbu geothermal field using numerical simulation. IOP Conference Series: Earth and Environmental Science, 1472, 012037.

Harrison, A.J. and Freeston, D.H., 1973. The calculation of steam–water flow in geothermal wells. In: *Proceedings of the Second United Nations Symposium on the Development and Use of Geothermal Resources*, San Francisco, USA, 20–29 May 1975. Washington, DC: U.S. Government Printing Office, pp.1459–1468.

Haukwa, C. B., & O'Sullivan, M. J. (1981). A study of cycling geothermal wells. Proceedings of the 3rd New Zealand Geothermal Workshop, 41–47.

Hewitt, G.F. and Hall-Taylor, N.S., 1970. *Annular two-phase flow*. Oxford: Pergamon Press.

Inagaki, M., Itoi, R., Kumagai, T., & Iwasaki, T. (2014). Numerical simulation on fluctuation in wellhead pressure of geothermal well. Proceedings, 39th Workshop on Geothermal Reservoir Engineering, Stanford University.

Jiménez Martínez, V.A. and Renner, J. (2022). Constraints on hydraulic properties from free pressure oscillations recorded during pumping operations in boreholes. *Geophysical Journal International*, 232(3), pp.1713–1741. doi:https://doi.org/10.1093/gji/ggac320.

Kurniawan, I., Sutopo, S., Pratama, H. B., & Adiprana, R. (2018). A natural state modelling of ulumbu geothermal field, east nusa tenggara, indonesia: An improved natural state model. Grand Renewable Energy 2018 Proceedings.

Li, H., Rane, S., & Yu, Z. (2021). Investigation of the performance and flow characteristics of two-phase reaction turbines in total flow geothermal systems. Renewable Energy,175, 345–372.

McGuinness, M. J. (2013). Correct energy conservation in geothermal wellbore simulation. Geothermics, 46, 1–9.

Moon, H., Situmorang, J., Azwar, L., & Franz, P. (2018). Numerical analysis of mcy01 production well mechanism: Understanding of well "coughing" phenomenon and irregular productivity. Proceedings, 43rd Workshop on Geothermal Reservoir Engineering. Stanford University, Stanford, California, February 12-14, 2018. SGP-TR-213

Moya, S. L., Aragon, A., Iglesias, E. R., & Santoyo, E. (1998). Prediction of mass deliverability from a single wellhead measurement and geothermal inflow performance reference curves. Geothermics, 27(3), 317–329.

Peng, L., Han, G., Chen, Z., Arnold Landjobo Pagou, Zhu, L. and Akhayie Mamat Abdoulaye (2022). Dynamically coupled reservoir and wellbore simulation research in two-phase flow systems: a critical review. *Processes*, 10(9), pp.1778–1778. doi:https://doi.org/10.3390/pr10091778.

Saptadji, N. M., Ashat, M. A., & Maulana, D. T. (2023). Teknik produksi geotermal. ITB Press.

Shulyupin, A. N. (2017). Steam–water flow instability in geothermal wells. International Journal of Heat and Mass Transfer, 107, 357–366.

Tonkin, R., O'Sullivan, J., & O'Sullivan, M. (2020). Development of a transient, multi-feed geothermal wellbore simulator. Proceedings World Geothermal Congress.

Wallis, G.B., 1969. *One-dimensional two-phase flow*. New York: McGraw-Hill.

Xu, T., Zhu, H., Feng, G., Yuan, Y., & Tian, H. (2017). On fluid and thermal dynamics in a heterogeneous co2 plume geothermal reservoir. Geofluids, 2017.

Yanto, E., Cici, K. E., Hastriansyah, G., Pasaribu, F., & Silaban, M. S. P. (2019). Managing the cycling effect on well ept-l/1. Proceedings 41st New Zealand Geothermal Workshop, 25-27 November 2019, Auckland, New Zealand.